Hindawi Publishing Corporation
Journal of Computer Networks and Communications
Volume 2016, Article ID 5680850, 14 pages
http://dx.doi.org/10.1155/2016/5680850

Research Article

The Impact of Noise Models on Capacity Performance of Distribution Broadband over Power Lines Networks

Athanasios G. Lazaropoulos

School of Electrical and Computer Engineering, National Technical University of Athens, Zografou Campus, 9 Iroon Polytechneiou Street, 15780 Athens, Greece

Correspondence should be addressed to Athanasios G. Lazaropoulos; aglazaropoulos@gmail.com

Received 28 November 2015; Revised 12 January 2016; Accepted 14 January 2016

Academic Editor: Tzonelih Hwang

This paper considers broadband potential of distribution Broadband over Power Lines (BPL) networks when different well-known noise models of the BPL literature are applied. The contribution of this paper is twofold. First, the seven most representative and used noise models of the BPL literature are synopsized in this paper. With reference to this set, the broadband performance of a great number of distribution BPL topologies either Overhead (OV) or Underground (UN), either Medium-Voltage (MV) or Low-Voltage (LV), is investigated in terms of suitable capacity metrics. Second, based on the proposed capacity metrics, a comparative capacity analysis is performed among various well-validated noise models. Through the careful study of its results, it is demonstrated that during capacity computations of distribution BPL networks, the flat Additive White Gaussian Noise (FL noise model) can be comfortably assumed as an efficient noise model either in 3–30 MHz or in 3–88 MHz frequency range since its capacity differences with the other well-proven noise models are negligible.

1. Introduction

The distribution power grids represent an omnipresent widely branched hierarchical structure. The deployment of BPL networks upon this structure defines the key to develop an advanced IP-based communications platform that may support a plethora of smart grid applications and broadband last mile access [1–9].

Utilities employ either OV or UN MTL configurations for new urban, suburban, and rural installations. When considered as a transmission medium for communications signals, OV and UN distribution power grids are subjected to various propagation and transmission deficiencies such as high and frequency-selective attenuation, EMI from/to other wireless services, and noise [1–4, 10–13]. Each of the aforementioned adverse factors critically influences the BPL network performance [14, 15].

Until now, a great number of attempts have been made in order to efficiently identify and describe the BPL noise characteristics [14–19]. Since various BPL noise features are very hard to be characterized through pure analytical derivations, the majority of the existing noise models are based on measurement approximations and practical rules [20]. Despite the increased number of investigators that deals with the thorny issue of BPL noise, there is need of simple but yet accurate noise models [20, 21]. Towards that direction, many BPL researchers tend to use simple but effective noise models that are proven to have realistic and experimentally verified results during capacity computations of distribution BPL networks in 3–30 MHz and 3–88 MHz frequency bands [16, 17, 22–28]. Depending on the countries authorities and their frequency regulations, these two frequency bands are available for the BPL applications and, hence, they are separately treated even though they have a common frequency range. In the same logic, during these capacity computations, an intuitive procedure among BPL engineers is the consideration of flat AWGN [2, 4, 11, 29]. The validity and the accuracy of the previous consideration are investigated with reference to other well-verified noise models presented in the BPL literature [15, 17, 22–28].

Valuable help towards the assessment of the broadband potential of distribution BPL networks offers the well established hybrid model, which has been extensively employed

to examine the behavior of various transmission and distribution BPL MTL structures [2–7, 29–31]. Synoptically, this hybrid model consists of (i) a bottom-up approach that is based on an appropriate combination of MTL theory and similarity transformations, such as EVDs and SVDs [6, 7, 29–33] and (ii) a top-down approach that is based on the concatenation of multidimensional T-matrices of distribution BPL network segments [2–6, 32]. The synthesis of the noise model, the hybrid model, and the elements of information theory determines the capacity of distribution BPL networks [2–5, 34]. Except for recognizing the role of BPL noise models, the capacity results of distribution BPL networks validate the significant the impact of the surrounding noise conditions on BPL performance [4, 11, 29, 35, 36].

The rest of this paper is organized as follows. In Section 2, the OV and UN distribution MTL configurations as well as their indicative topologies are presented. Section 3 summarizes the principles of BPL signal propagation through the lens of the well-validated hybrid model: MTL theory, EVD modal analysis, and the coupling scheme concerning the injection of BPL signals into the power lines. Section 4 synopsizes the main factors that influence BPL capacity; say, EMI policies and noise characteristics. Special attention is given to the noise models that are available from the BPL literature and are examined in this paper. In Section 5, numerical results and discussion are provided in order to highlight the significant role of noise and noise models during BPL capacity computations. Section 6 concludes this paper.

2. Distribution Power Grids

In this section, first, a brief presentation of the distribution MTL configurations (i.e., OV MV, OV LV, UN MV, and UN LV MTL configurations) is given. Second, the indicative distribution topologies, which are used in the following analysis, are reported.

2.1. OV MV MTL Configurations. A typical case of OV MV distribution line is depicted in Figure 1(b). OV MV distribution lines hang at typical heights $h_{\mathrm{MV}}^{\mathrm{OV}}$ above the ground. Typically, three parallel noninsulated phase conductors spaced by $\Delta_{\mathrm{MV}}^{\mathrm{OV}}$ reused the above lossy ground. This three-phase three-conductor ($n^{\mathrm{OV\,MV}} = 3$) OV MV distribution line configuration is considered in the present work, consisting of ACSR $3 \times 95\,\mathrm{mm}^2$ conductors. The aforementioned exact dimensions are reported in [2, 6, 29, 35–37].

The ground is considered as the reference conductor either for OV MV or for OV LV MTL configuration. In all the cases examined, the values of the ground conductivity σ_g and ground relative permittivity ε_{rg} are detailed in [2, 29, 35]. The impact of imperfect ground on signal propagation via OV power lines was analyzed in [2–5, 29, 35, 36, 39, 40].

2.2. UN MV MTL Configurations. The UN MV distribution line that will be examined is the three-phase sector-type PILC distribution-class cable (8/10 kV, $3 \times 95\,\mathrm{mm}^2$ Cu, PILC) and illustrated in Figure 1(d). The cable arrangement consists of the three-phase three-sector-type conductors ($n^{\mathrm{UN\,MV}} = 3$), one shield conductor, and one armor conductor. The shield and the armor are grounded at both ends. Details regarding conductors, shield, armor, and insulation dimensions are provided in [3, 6, 17, 41].

As it is concerned with the propagation mechanisms across UN MV and UN LV MTL configurations of this paper, due to the common practice of grounding at both ends, the shield acts as a ground return path and as a reference conductor. Hence, the analysis of UN distribution configurations can be focused only on the inner MTL sets consisting of [5, 6, 37, 42] (i) the three phases; (ii) the shield; and (iii) the neutral conductor (only in the case of UN LV BPL MTL structure presented in Section 2.4) [3, 17, 30, 32, 37, 41]. The analytical formulation, which is adopted in this paper for UN distribution BPL systems, considers high frequency BPL transmission in the general case of UN power lines consisting of multiple conductors with common shield [3–5, 30, 32, 42, 43].

2.3. OV LV MTL Configurations. A typical case of OV LV distribution line is depicted in Figure 1(a). Four parallel noninsulated conductors are suspended one above the other spaced by $\Delta_{\mathrm{LV}}^{\mathrm{OV}}$ and located at heights $h_{\mathrm{LV}}^{\mathrm{OV}}$ above the ground for the lowest conductor. The upper conductor is the neutral, while the lower three conductors are the three phases. This three-phase four-conductor ($n^{\mathrm{OV\,LV}}$) OV LV distribution line configuration consists of ASTER $3 \times 54.6\,\mathrm{mm}^2 + 134.4\,\mathrm{mm}^2$ conductors. The aforementioned exact dimensions are detailed in [6].

2.4. UN LV MTL Configurations. The UN LV distribution line that is examined in this paper is the three-phase four-conductor ($n^{\mathrm{UN\,LV}} = 4$) core-type UN LV distribution cable ($4 \times 25\,\mathrm{mm}^2$ Cu, XLPE) buried inside the ground. The layout of this cable is depicted in Figure 1(c). This cable arrangement consists of the three-phase three-core-type conductors, one core-type neutral conductor, and one shield conductor. Details regarding conductors, shield, and insulation dimensions are provided in [5, 30, 32, 37, 42].

2.5. Indicative OV and UN Distribution BPL Topologies. The generic BPL topology of Figure 2(a) is considered for the BPL topologies of this paper. This topology is bounded by the transmitting and the receiving ends while having N branches. To apply the hybrid model, an end-to-end BPL topology is separated into segments (network modules), each of them comprising the successive branches encountered [6]. In accordance with [2–6, 17, 29, 32, 35, 37, 44], the average path lengths in the order of 1000 m and 200 m are considered in OV and UN distribution BPL topologies, respectively.

As it is concerned with OV distribution BPL topologies, the five indicative OV distribution BPL topologies of [6] concerning the end-to-end connections of average path lengths are also considered in this paper. These indicative topologies, which are common for both OV MV and OV LV BPL networks, are (i) a typical urban topology (OV MV or OV LV urban case A); (ii) an aggravated urban topology

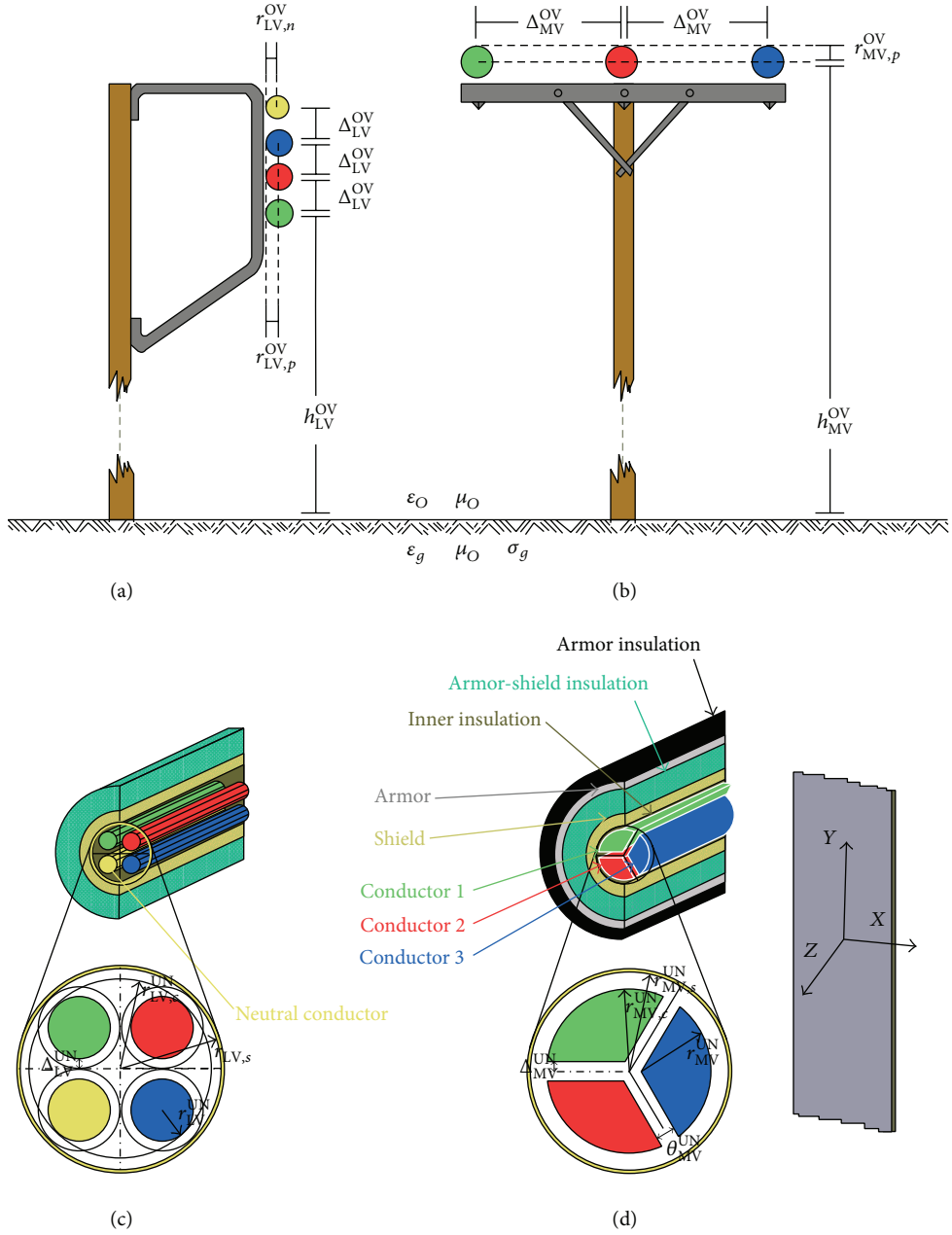

FIGURE 1: Typical multiconductor structures [38]. (a) Overhead LV. (b) Overhead MV. (c) Underground LV. (d) Underground MV.

(OV MV or OV LV urban case B); (iii) a typical suburban topology (OV MV or OV LV suburban case); (iv) a typical rural topology (OV MV or OV LV rural case); and (v) the LOS transmission along the same end-to-end distance $L = L_1 + \cdots + L_{N+1} = 1000$ m. This topology corresponds to Line of Sight transmission in wireless channels.

Similar to OV distribution BPL topologies, five indicative UN distribution BPL topologies, which concern average long end-to-end connections of 200 m that are detailed in [2, 4, 6], are examined in this paper. As in OV distribution BPL case, the UN distribution BPL topologies are common for both MV and UN networks.

With reference to Figure 2(b), the circuital parameters of the above indicative OV and UN distribution BPL topologies are detailed in [2–6, 17, 29, 32, 35, 37, 44]. Synoptically, the branching cables are assumed to be identical to the distribution cables and the interconnections between the distribution and branch conductors are fully activated. The transmitting and the receiving ends are assumed to match the characteristic impedance of the modal channels, whereas the branch terminations are assumed to be open circuit.

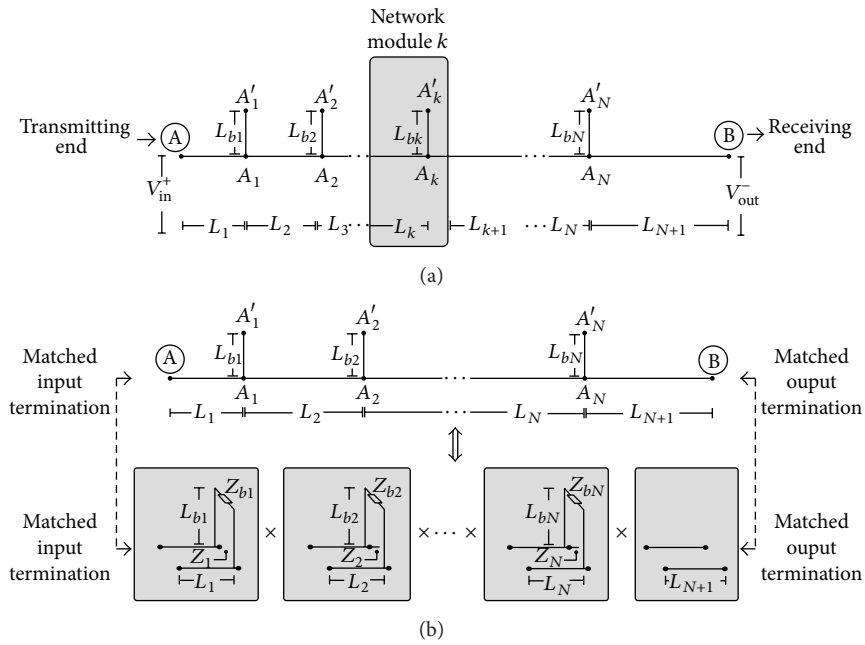

FIGURE 2: (a) End-to-end BPL connection with N branches. (b) An indicative BPL topology considered as a cascade of modules corresponding to N branches [6].

3. The Principles of BPL Transmission Analysis

In this section, a brief presentation of the fundamental principles during the BPL signal propagation and transmission is given. First, MTL theory that describes the BPL signal propagation across the examined MTL configurations is presented. Then, EVD modal analysis and practical coupling schemes that describe BPL signal transmission through the indicative distribution topologies are outlined.

3.1. MTL Theory and EVD Modal Analysis. Already presented in [2–6], through a matrix approach, the standard TL analysis that involves two conductors can be extended to the MTL analysis, which involves more than two conductors. Compared to a two-conductor line supporting one forward- and one backward-traveling wave, an MTL structure with $n^G + 1$ conductors parallel to the z-axis may support n^G pairs of forward- and backward-traveling waves with corresponding propagation constants, where $[\cdot]^G$ denotes the examined power grid type, that is, either OV MV or UN MV or OV LV or UN LV. Each pair of forward- and backward-traveling waves is referred to as a mode. The modes, supported by the aforementioned MTL configurations, propagate across the BPL topologies, while their spectral behavior is analytically investigated in [2–6, 29, 30, 32, 33, 35–37, 39, 40].

TM2 method, which is based on the scattering matrix theory [2–6, 30–32] and presented analytically in [6], models the spectral behavior of these n^G modes proposing the $n^G \times n^G$ EVD modal transfer function matrix $\mathbf{H}^m\{\cdot\}$ whose elements $H_{i,j}^m\{\cdot\}$, $i, j = 1, \ldots, n^G$ are the EVD modal transfer functions where $H_{i,j}^m$ denotes the element of matrix $\mathbf{H}^m\{\cdot\}$ in row i of column j.

3.2. OV and UN Distribution BPL Networks and Practical Coupling Schemes. In accordance with [2, 6, 29, 35], there are two different coupling schemes that may inject signals into OV distribution BPL networks, namely, (i) WtG coupling schemes when the signal is injected into one conductor and returns via the ground and (ii) WtW coupling schemes when the signal is injected between two conductors. Similar to OV distribution BPL networks, there are two different coupling schemes for UN distribution BPL networks, namely, (i) StP coupling schemes when the signal is injected into one conductor and returns via the shield and (ii) PtP coupling schemes when the signal is injected between two conductors.

WtG or StP coupling between conductor s and ground or shield will be detoned by WtG^s or StP^s, respectively, whereas WtW or PtP coupling between conductors p and q will be detoned by $\mathrm{WtW}^{p\text{-}q}$ or $\mathrm{PtP}^{p\text{-}q}$, respectively.

As it has already been determined in [5, 6, 29], since EVD modal transfer function matrix $\mathbf{H}^m\{\cdot\}$ is well-defined by TM2 method, the coupling transfer function $H^C\{\cdot\}$ is given from

$$H^C\{\cdot\} = \left[\mathbf{C}^C\right]^T \cdot \mathbf{T}_V \cdot \mathbf{H}^m\{\cdot\} \cdot \mathbf{T}_V^{-1} \cdot \mathbf{C}^C, \quad (1)$$

where $[\cdot]^T$ denotes the transpose of a matrix, $[\cdot]^C$ denotes the applied coupling scheme, $\mathbf{C}^C$ is the $n^G \times 1$ coupling column vector detailed in [3, 33, 35], and $\mathbf{T}_V$ is $n^G \times n^G$ matrix depending on the frequency, the power grid type, the physical properties of the cables, and the geometry of the MTL configuration [2–6].

4. EMI Policies, Noise, and Capacity of OV and UN Distribution BPL Networks

In this section, the factors, such as EMI policies and noise, that influence the capacity of a BPL network are outlined.

4.1. EMI Policies. To regulate the emissions from BPL networks to other already licensed radiocommunications systems in the same frequency band of operation, a great number of regulatory bodies have established proposals (EMI policies) concerning the electromagnetically safe BPL operation. The IPSD limits proposed by Ofcom for compliance with FCC Part 15 are adopted in this paper. Ofcom's IPSD limits, which are analytically discussed in [45–47] assume that the maximum levels of −60 dBm/Hz and −40 dBm/Hz constitute appropriate IPSD limits $p(f)$ for OV and UN BPL networks, respectively, in the 3–30 MHz frequency range providing presumption of compliance with the current FCC Part 15 limits. Similarly, in the 30–88 MHz frequency range, Ofcom's IPSD limits assume that maximum IPSD limits $p(f)$ that are equal to −77 dBm/Hz and −57 dBm/Hz for OV and UN BPL networks, respectively, may provide the required EMI compliance. Without losing the generality of the analysis, a typical procedure is the consideration of common IPSD limits for OV and UN distribution BPL networks regardless of the power grid level, that is, either MV or LV, exploiting the significant similarities regarding OV and UN BPL signal propagation, respectively.

4.2. Noise. As it has already been demonstrated in [2–6, 16–20], all today's available BPL noise models are obtained based on either frequency-domain or time-domain empirical measurements.

In general, BPL noise may be considered as an appropriate superposition of five noise types, which are distinguished by their origin, intensity, spectrum occupancy, and time duration [14–17, 20, 22–28]. Regardless of the power grid type, either OV or UN, either MV or LV, these five types of noise are (i) the colored background noise; (ii) the narrowband noise; (iii) the periodic impulsive noise asynchronous to the mains frequency; (iv) the periodic impulsive noise synchronous to the mains frequency; and (v) the asynchronous impulsive noise. Since the first two types of noise present a quasi-stationary behavior either in frequency-domain or in time-domain, they can be jointly treated as background noise. On the other hand, the last three types can be considered as impulsive noise since their behaviors present significant fluctuations over short periods of time, time periods, and locations either in frequency-domain or in time-domain.

As concerns the available modeling approaches, the background noise is preferably modeled in the frequency-domain, whereas the impulsive noise can be satisfactorily described either in frequency-domain or in time-domain. Despite the significantly diverse behavior of impulsive noise, a decent number of proper countermeasure techniques seem to cope with this significant BPL burden, hopefully [24–26, 48].

Anyway, as it is widely used during capacity computations in BPL networks [2, 4, 29, 34–36], only the nonresolvable limitations that are common in all BPL networks should be considered. Since the background noise is the only consistent noise in BPL networks, only its behavior is examined in the following capacity analysis. In order to model the background noise in the frequency-domain, the dominant method is the spectrum fitting where the measured noise PSD is fitted into certain functions of frequency. This method captures the average noise spectrum [7, 10, 14, 15, 19, 20, 22–27].

Regardless of the power grid type, general observations of background noise in the 3–30 MHz and 3–88 MHz frequency bands reveal that its noise PSD is higher at lower frequencies. As frequency increases, noise PSD of background noise reduces and smoothly decays to spectrally flat AWGN above a specific frequency (denoted by threshold frequency). At high frequencies, it can be assumed that the noise is spectrally flat AWGN [17, 24–28]. To mathematically describe this noise PSD, a first-order exponential function is more adequate as formulated by [15, 22, 23]

$$N(f) = N_{NF} + n_1 \cdot e^{-n_2 \cdot f}, \tag{2}$$

where f is the frequency in MHz, N_{NF} is the spectrally flat AWGN/PSD expressed in dBm/Hz, and n_1 and n_2 are the exponential coefficients of the noise model.

Already mentioned in [2–6], as regards the AWGN properties of distribution BPL networks either in the 3–30 MHz or in the 3–88 MHz frequency range, the AWGN/PSD levels N_{NF} are considered equal to −105 dBm/Hz and −135 dBm/Hz in the case of OV and UN distribution BPL networks, respectively, which is a realistic scenario [2–6, 14, 15, 17–19, 29, 34, 35, 45]. Apart from these values that represent the average AWGN noise type, AWGN/PSD levels that vary from −15 dB (noise type A) to +15 dB (noise type B) are assumed; noise type A and noise type B represent the good and the bad noise scenarios, respectively, and this 30 dB variance may give a representative image of the intensity and variety of noise conditions that occur in different noise environments across practical distribution BPL networks (for more details, see [2–6, 34]).

Depending on the values of their exponential coefficients, seven well-known noise models have been selected from the literature and are compared in this paper. More specifically, one can find

(1) the spectrally flat AWGN noise model where n_1 and n_2 are equal to zero (denoted by FL noise model and proposed in [2, 4, 11, 29, 34–36]);

(2) the OPERA proposal where n_1 and n_2 are equal to 24.613 dB and 0.105 MHz^{-1}, respectively (denoted by OPERA noise model and presented in [17]);

(3) the noise model presented in [24, 25, 27, 28] where n_1 and n_2 are equal to 75 dB and 2 MHz^{-1}, respectively (denoted by MEN noise model);

(4) the first noise model presented in [15, 22, 23] where n_1 and n_2 are equal to 35 dB and 0.2778 MHz^{-1}, respectively (denoted by PH1 noise model). This model is primarily suitable for residential noise environments;

(5) the second noise model presented in [15, 22, 23] where n_1 and n_2 are equal to 40 dB and 0.1163 MHz^{-1},

respectively (denoted by PH2 noise model). This model mainly characterizes industrial noise environments;

(6) the first noise model presented in [26] where n_1 and n_2 are equal to 38.75 dB and 0.72 MHz^{-1}, respectively (denoted by ESM1 noise model);

(7) the second noise model presented in [26] where n_1 and n_2 are equal to 53.23 dB and 0.337 MHz^{-1}, respectively (denoted by EMS2 noise model).

Similar to IPSD limits, common noise characteristics are assumed for OV distribution BPL networks regardless of the power grid level, which is a rather common procedure. The same assumption occurs for UN distribution BPL networks.

4.3. Capacity. Capacity is defined as the maximum achievable transmission rate that can be reliably transmitted over a BPL network, whereas cumulative capacity is the cumulative upper limit of information, which can be reliably transmitted over a BPL network. According to [1–6], both these spectral metrics depend on the applied MTL configuration, the type of power grid, the power grid topology, the coupling scheme applied, the adopted EMI policies, and the noise environment.

Based on (1) and (2) and with reference to Figure 2(a), the capacity C of a distribution BPL network is determined by [2, 4, 29]

$$C = C_{\text{A}\to\text{B}}^{\text{SISO}} = f_s \cdot \sum_{q=0}^{Q-1} \log_2 \cdot \left\{ 1 + \left[\frac{\langle p(qf_s)\rangle_L}{\langle N(qf_s)\rangle_L} \cdot \left| H^C(qf_s) \right|^2 \right] \right\}, \quad (3)$$

where $[\cdot]_{\text{A}\to\text{B}}$ determines the transmitting (A) and receiving (B) end point, $\langle\cdot\rangle_L$ is an operator that converts dBm/Hz into a linear power ratio (W/Hz), Q is the number of subchannels in the BPL signal frequency range of interest, and f_s is the flat-fading subchannel frequency spacing.

5. Numerical Results and Discussion

The numerical results of various types of OV and UN distribution BPL networks aim at investigating (a) their BPL capacity performance; (b) the influence of different noise environments on the capacity performance; and (c) the role of noise models.

As it is concerned with the following capacity analysis, only one representative configuration of each coupling scheme—say, WtG^1, $\text{WtW}^{1\text{-}2}$, StP^1, and $\text{PtP}^{1\text{-}2}$ coupling schemes—will be examined in the rest of this paper. This common assumption does not affect the generality of the following BPL capacity analysis [1, 5, 6].

5.1. Remembering the Influence of Different Noise Environments on OV and UN Distribution BPL Network Capacity. As it has first been identified in [2, 4, 8, 9, 11, 13, 29, 34–36, 38], to establish high-bitrate data communications with capacities in the range of Gbps in distribution BPL networks, the elaborated examination of the inherent BPL deficiencies is required. Among them, the impact of noise on BPL performance is critical, since BPL noise nature is highly variable [2–4, 11, 12, 14–19, 22–29, 35, 36, 45]. The detailed knowledge of the noise properties in the mainstream BPL operation bands, that is, 3–30 MHz and 3–88 MHz frequency ranges, may contribute towards the design of more efficient modulation and coding schemes suitable for BPL networks.

The following subsection assesses the impact of noise environments on the capacity of OV and UN distribution BPL networks. In order to assess the effect of different noise environments on BPL capacity, apart from the average noise type, noise type A, and noise type B, which have been presented in Section 4.2, are assumed. In this subsection, for simplicity, only the FL noise model is applied.

In Figure 3(a), the cumulative capacity is plotted versus the frequency in the 3–88 MHz frequency band for the indicative OV MV BPL topologies, presented in Section 2.5, when WtG^1 coupling scheme is applied. In Figures 3(b)–3(d), similar curves are given in the case of UN MV, OV LV, and UN LV BPL topologies, respectively, when StP^1, WtG^1, and StP^1 coupling schemes are applied, respectively.

In Figures 4(a)–4(d), similar plots to Figures 3(a)–3(d) are drawn in the case of $\text{WtW}^{1\text{-}2}/\text{PtP}^{1\text{-}2}$ coupling schemes.

Figures 3(a)–3(d) and 4(a)–4(d) show the significance of noise in today's distribution BPL network performance [14, 15]. In all the cases examined, capacity differences of the order of hundreds of Mbps are observed when different noise conditions occur. Actually, a 15 dB increase of noise PSD (noise type B) in the 3–88 MHz frequency band corresponds to an average capacity reduction equal to 396 Mbps, 288 Mbps, 396 Mbps, and 429 Mbps for OV MV, UN MV, OV LV, and UN LV BPL networks, respectively, when $\text{WtG}^1/\text{StP}^1$ coupling schemes are applied. Similarly, in the case of $\text{WtW}^{1\text{-}2}/\text{PtP}^{1\text{-}2}$ coupling schemes, when the same increase of noise PSD occurs, average capacity reductions equal to 360 Mbps, 260 Mbps, 359 Mbps, and 429 Mbps are observed for OV MV, UN MV, OV LV, and UN LV BPL networks, respectively.

Based on this short collection of capacity observations, a rule of thumb suggests that each dB of increase above average noise PSD corresponds to a capacity reduction that approximately ranges from 17.3 Mbps to 28.6 Mbps in the 3–88 MHz frequency band. Its exact value depends on the used frequency band, power grid type, BPL topology, and applied coupling scheme. Anyway, relative capacity results occur when 3–30 MHz frequency band and/or noise type A are adopted.

In addition, comparing capacity results between $\text{WtG}^1/\text{StP}^1$ coupling schemes and their respective $\text{WtW}^{1\text{-}2}/\text{PtP}^{1\text{-}2}$ ones for given power grid type and BPL topology, their capacity differences are negligible indicating the strongly deteriorative nature of noise regardless of the coupling scheme applied, BPL topology, and power grid type. Since the destructive role of noise is ubiquitous, only $\text{WtG}^1/\text{StP}^1$ coupling schemes are adopted in the following analysis due to their representative capacity results.

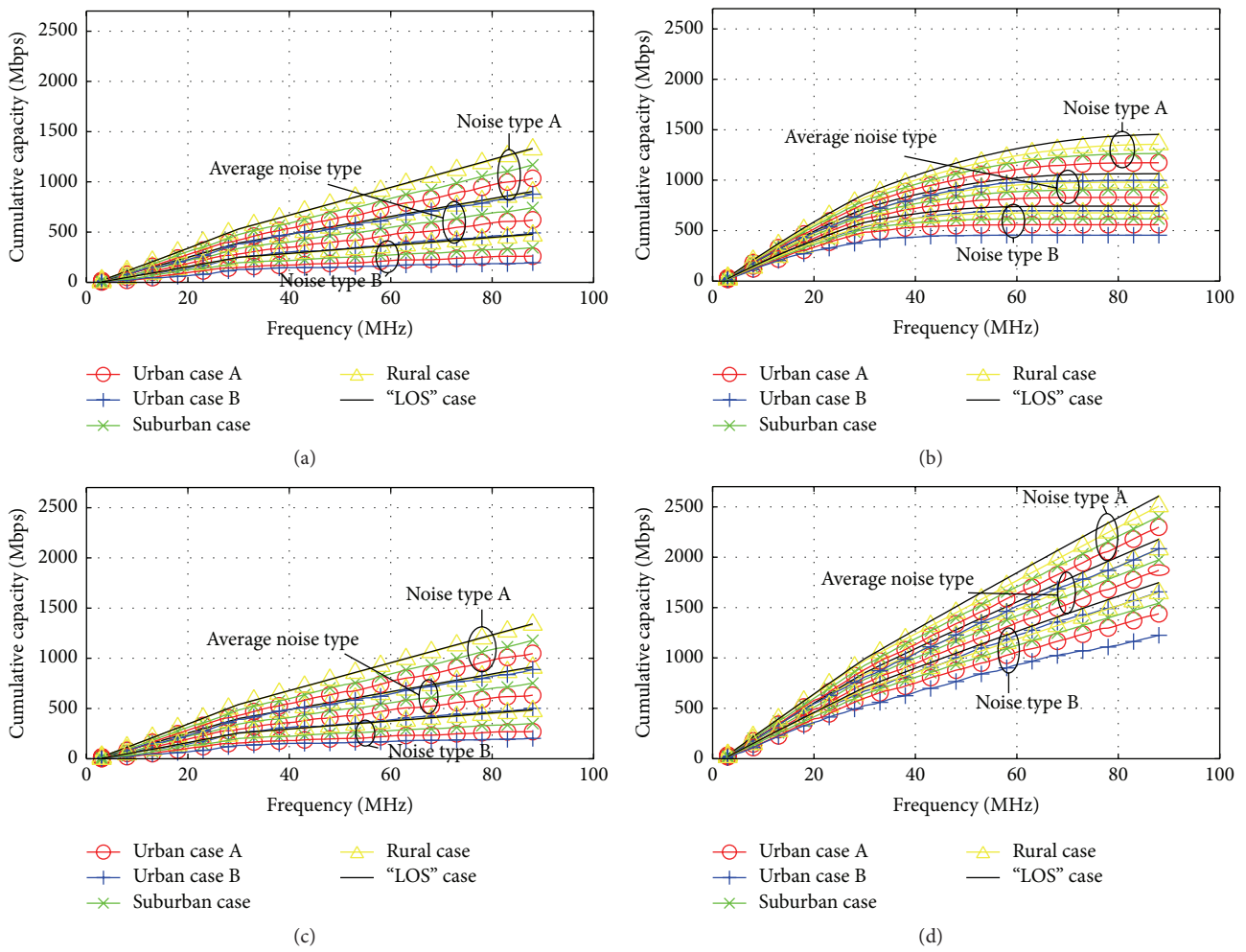

Figure 3: Cumulative capacity versus frequency of the indicative topologies of distribution BPL networks in the 3–88 MHz frequency band when WtG[1]/StP[1] coupling schemes are deployed and FCC Part 15 is adopted. Noise type A, average noise type, and noise type B are considered. (a) OV MV/WtG[1]. (b) UN MV/StP[1]. (c) OV LV/WtG[1]. (d) UN LV/StP[1].

5.2. The Role of Noise Models during Capacity Computation of OV and UN Distribution BPL Networks. Observing Figures 3(a)–3(d) and 4(a)–4(d), the fact that today's OV and UN distribution BPL networks resemble high-capacity transmission systems shows an attractive broadband last mile solution and reliable candidate broadband technology for the oncoming smart grid [2, 4, 6, 7, 11, 29, 35, 36]. However, despite these relatively favourable capacity characteristics, according to the picture obtained from their capacity behavior, the influence of noise still remains crucial for the widespread adoption of BPL technology. Due to its multi-Mbps impact, the application of efficient and simple noise models defines the accuracy of capacity computations.

To investigate the effect of different noise models on BPL capacity performance, a set of numerical results concerning capacities of OV and UN distribution BPL networks in the 3–30 MHz and 3–88 MHz frequency ranges is demonstrated in this subsection. Across this subsection, only the average noise type is adopted without, however, affecting the generality of BPL capacity analysis concerning the influence of BPL noise models.

At the same time, the potential of using the simpler noise model proposals, such as FL one, without, however, affecting the capacity computation accuracy is investigated in this subsection. This is a crucial matter during capacity computations because the low degree of complexity of FL noise model permits simpler and straightforward source codes that further imply high computation speed during simulation results.

Indeed, in Figures 5(a)–5(g), the cumulative capacity is plotted versus frequency for the indicative OV MV BPL topologies when the seven aforementioned noise models of Section 4.2 are applied, respectively. In the same figures, the CCPC between the respective noises models and the FL one is presented. In Figures 6(a)–6(g), 7(a)–7(g), and 8(a)–8(g), same plots are given in the case of UN MV, OV LV, and UN LV BPL networks, respectively.

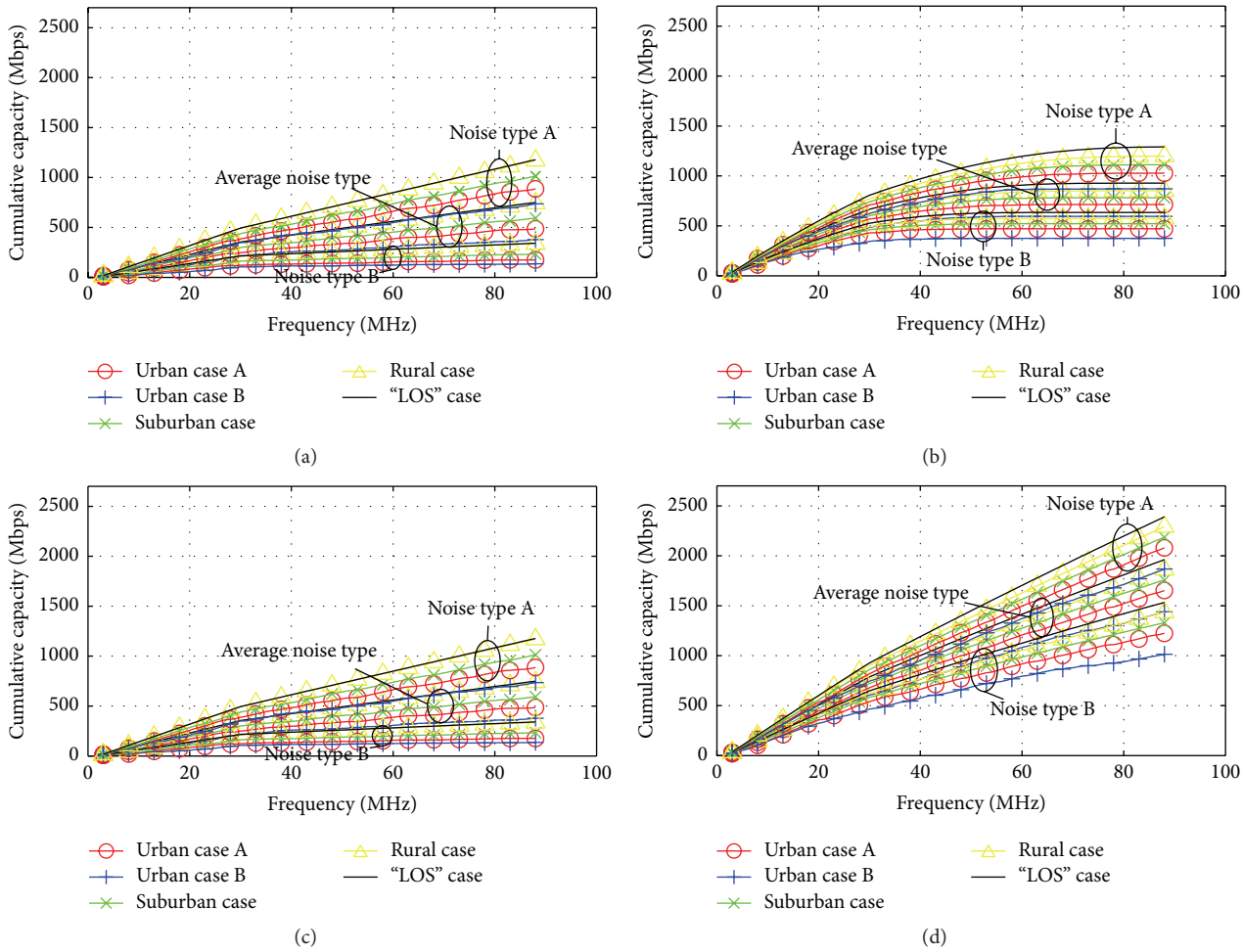

FIGURE 4: The same as in Figure 3, but for WtW$^{1\text{-}2}$/PtP$^{1\text{-}2}$ coupling schemes. (a) OV MV/WtW$^{1\text{-}2}$. (b) UN MV/PtP$^{1\text{-}2}$. (c) OV LV/WtW$^{1\text{-}2}$. (d) UN LV/PtP$^{1\text{-}2}$.

From Figures 5(a)–5(g), 6(a)–6(g), 7(a)–7(g), and 8(a)–8(g), the following interesting remarks are pointed out.

(i) With reference to [24–28], the noise characteristics of BPL networks can successfully be described from a few hundred kHz up to 100 MHz using the aforementioned BPL noise models. In accordance with their outcomes presented in the previous figures, in the majority of the cases examined, for frequencies less than a frequency threshold, distribution BPL networks suffer from correlated noise with a nonwhite profile. This frequency threshold strongly depends on power grid type but, in all the cases examined, it ranges from 10 MHz to 25 MHz. For frequencies above the frequency threshold, noise tends to follow the more commonly AWGN approximation (FL noise models) in all BPL networks regardless of power grid type and BPL topology. Practically, this is validated by the CCPC curves where the convergence of all the well-known models with the FL one is speeded up at high frequencies.

(ii) Due to the favourable propagation characteristics of UN distribution BPL networks (i.e., significantly higher IPSD limits, lower noise PSD, and shorter average end-to-end transmission distances), it is evident that the different noise models affect in a less way the capacity computations of UN distribution BPL networks in comparison with respective OV ones. Regardless of the power grid level, the capacity results of all noise models tend to coincide with the UN frequency threshold that is equal to 10 MHz. Similarly, OV distribution BPL networks present the same behavior with UN ones but for OV frequency threshold, which is obviously higher in comparison with UN one that is equal to approximately 20–25 MHz.

(iii) Comparing Figures 5(a)–5(g), 6(a)–6(g), 7(a)–7(g), and 8(a)–8(g) with Figures 3(a)–3(d) and 4(a)–4(d), it is clearly shown that the capacity impact of disturbed noise environments is significantly stronger compared to the capacity differences observed among

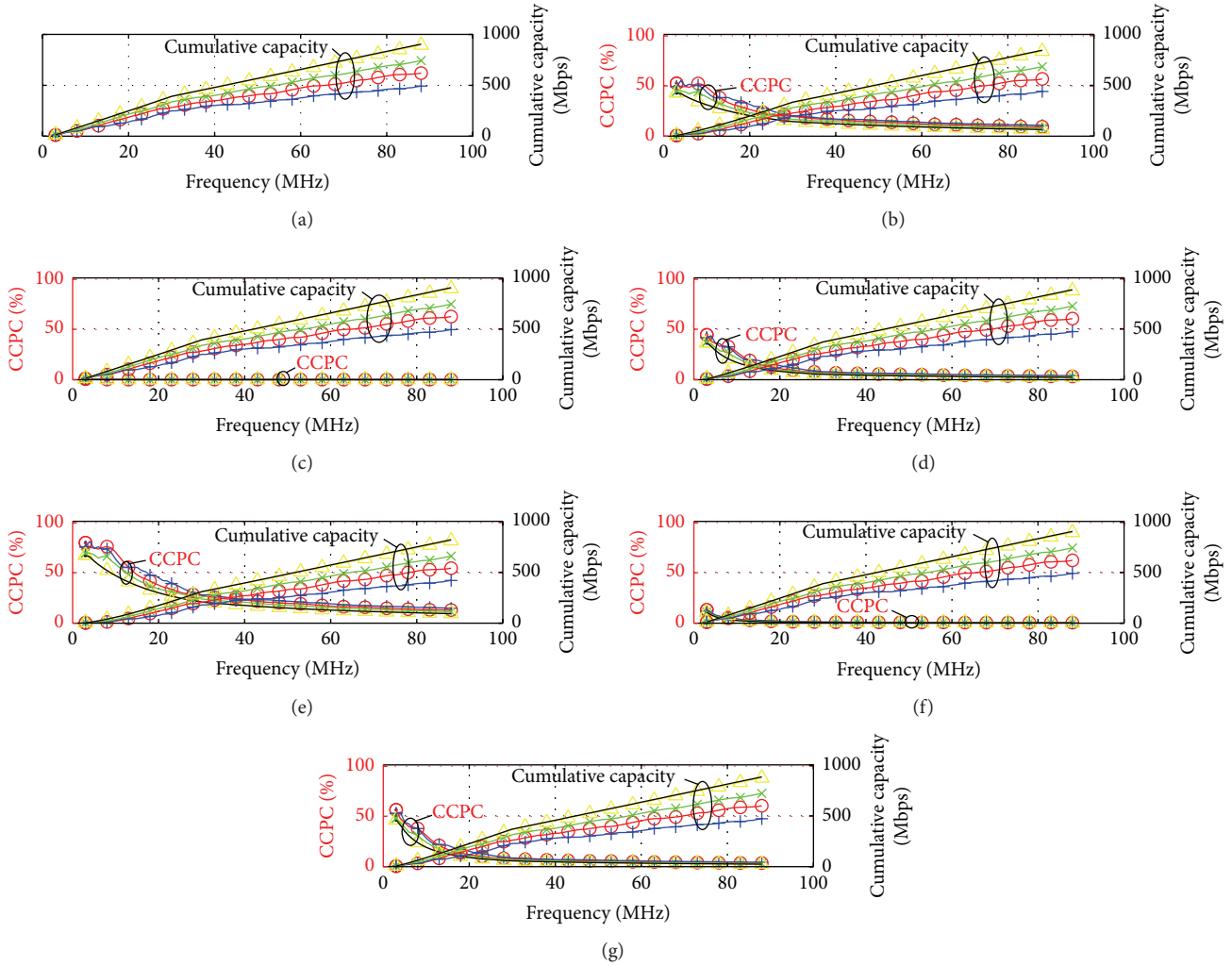

FIGURE 5: Cumulative capacity and CCPC versus frequency of the indicative topologies of OV MV BPL networks, urban case A (red circle), urban case B (blue cross), suburban case (green star), rural case (yellow triangle), and LOS case (black line), in the 3–88 MHz frequency band for the seven aforementioned noise models when respective WtG^1/StP^1 coupling schemes are deployed, average noise type is assumed, and FCC Part 15 is adopted. (a) FL noise model (with no CCPC curves). (b) OPERA noise model. (c) MEN noise model. (d) PH1 noise model. (e) PH2 noise model. (f) ESM1 noise model. (g) ESM2 noise model.

the seven aforementioned noise models in the 3–88 MHz frequency band; each dB of PSD noise increase corresponds to an average 23 Mbps capacity loss whereas the average overall capacity difference due to the adoption of different noise models is less than 20 Mbps.

(iv) The above capacity analysis in terms of cumulative capacity and CCPC ascertains a general noise belief that has been subliminally reproduced among BPL researchers for years [2, 4, 11, 29, 34–36]; FL noise model may be comfortably used during capacity computations of all OV and UN distribution BPL networks in the 3–88 MHz frequency band since the capacity differences among all available noise models are negligible in this frequency band of BPL operation. However, the straightforward adoption of FL noise model needs more explanations in the 3–30 MHz frequency band: although FL noise model gives accurate results in all the UN distribution BPL networks examined, in OV distribution BPL networks, FL noise model seems to satisfactorily describe the majority of noise environments, but not all. Actually, FL noise model seems to present some capacity deviations near industrial environments where noise PSD present high value at lower frequencies; see PH2 noise model of Figures 5(e) and 7(e). Nevertheless, even in these disturbed noise cases, the capacity differences among different noise models, which are approximately equal to 30 Mbps, present lower values than the respective capacity aggravation due to disturbed noise environments themselves, which are approximately equal to 280 Mbps for noise type

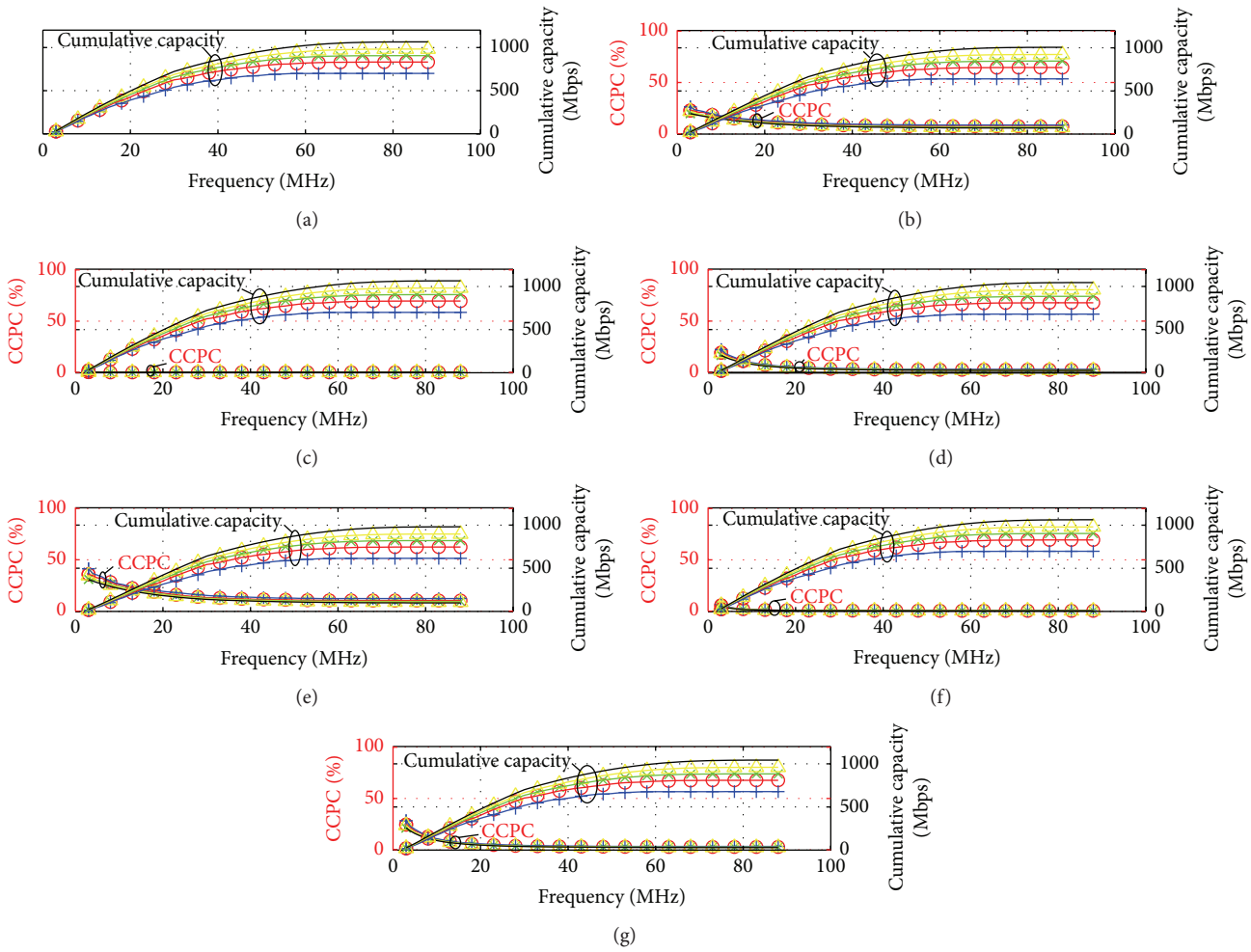

Figure 6: The same as in Figure 5, but for UN MV BPL networks.

B. Therefore, the FL noise model may be safely used during capacity computations of all distribution BPL networks either in 3–30 MHz or in 3–88 MHz frequency bands.

(v) As already mentioned, the use of the simple FL noise model can also lead to a straightforward source code with high computational speed. Indeed, in Figure 9, the execution time needed for the simulations of Figures 5–8 is plotted versus the flat-fading subchannel frequency spacing when different noise models are adopted in the 3–88 MHz frequency range. The execution time of the other noise models except FL one coincides since they are all based on (2). Conversely, FL noise model uses only the constant term of (2) bypassing the time consuming exponential function. As the required accuracy of simulations increases, the subchannel frequency spacing decreases leading to significant execution time differences between the FL noise model and the other ones. In fact, when the frequency spacing is equal to 1 Hz, the time difference reaches up to 48.12 s. As it is concerned with the technical characteristics of the system performing the simulations, it has an Intel Pentium 1.9 GHz CPU and 4 GB RAM.

(vi) More accurate and simpler noise models offer an important elementary step towards the design/operation of faster and more interoperable/intraoperable BPL systems in the (i) oncoming smart grid network and (ii) future M2M communications networks [49, 50]. Their presence defines the role of bridge among different OV and UN distribution BPL networks. Anyway, BPL noise models can be selfsame and straightforward and can be considered as available middleware tool in future BPL networks.

6. Conclusions

This paper has focused on the broadband potential of distribution BPL networks associated with the presence of different noise environments and noise models.

Based on the results of spectral metrics such as cumulative capacity and CCPC, major features of OV MV, UN MV,

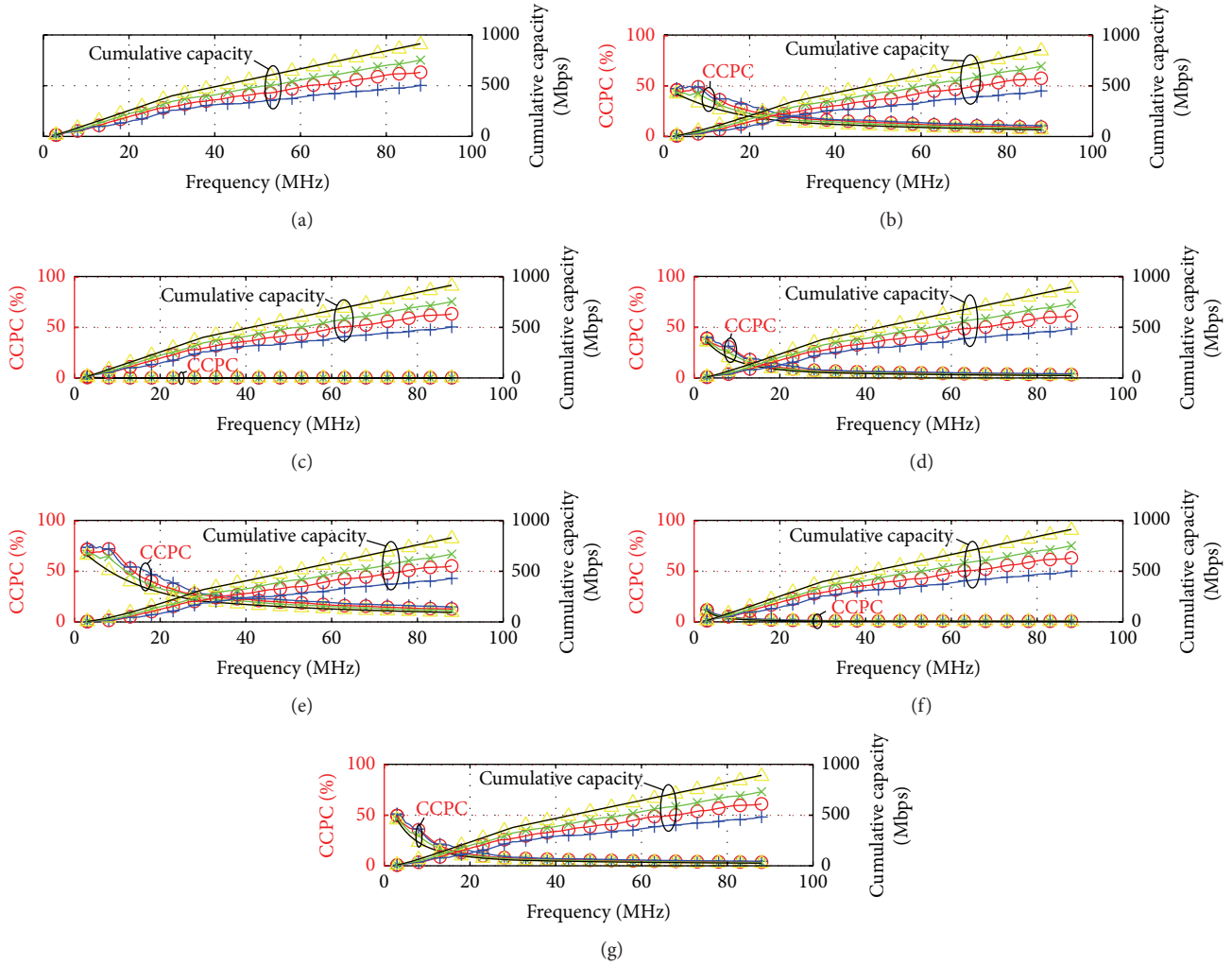

Figure 7: The same as in Figure 5, but for OV LV BPL networks.

OV LV, and UN LV BPL networks concerning their noise dependence have been reviewed. In the light of information theory, it has been verified that the capacity performance of distribution BPL networks is dramatically affected by their surrounding noise conditions. Actually, the capacity impact of noise is so severe that a slight increase of noise PSD in the order of few dBs may skyrocket capacity losses up to tens of Mbps regardless of the coupling scheme applied. Hence, noise has been identified as a leading inherent BPL deficiency that may severely degrade the BPL capacity performance.

Therefore, due to the high importance of noise modeling, the development of simple and accurate noise models is imperative. Towards that direction, FL noise model, that is the abbreviated name of the spectrally flat AWGN noise model, has been proven to be an efficient and precise tool for computing the capacities of distribution BPL networks in the 3–30 MHz and 3–88 MHz frequency ranges, which are the mainstream BPL operation frequency bands. Actually, FL noise model exploits the converging behavior of all the well-validated BPL noise models in the above frequency bands, simplifying, thus, today's strict capacity computation guidelines and the existence of high complexity during source code development.

Nomenclature

ACSR:	Aluminium Conductor Steel-Reinforced
AWGN:	Additive White Gaussian Noise
BPL:	Broadband over Power Lines
CCPC:	Cumulative Capacity Percentage Change
EMI:	ElectroMagnetic Interference
EVD:	Eigen Value Decomposition
IPSD limits:	Injected Power Spectral Density limits
LoS:	Line of Sight
LV:	Low-Voltage
M2M:	Machine-to-Machine
MTL:	Multiconductor Transmission Line
MV:	Medium-Voltage
OV:	Overhead
PILC:	Paper-Insulated Lead-Covered
PSD:	Power Spectral Density
PtP:	Phase-to-Phase

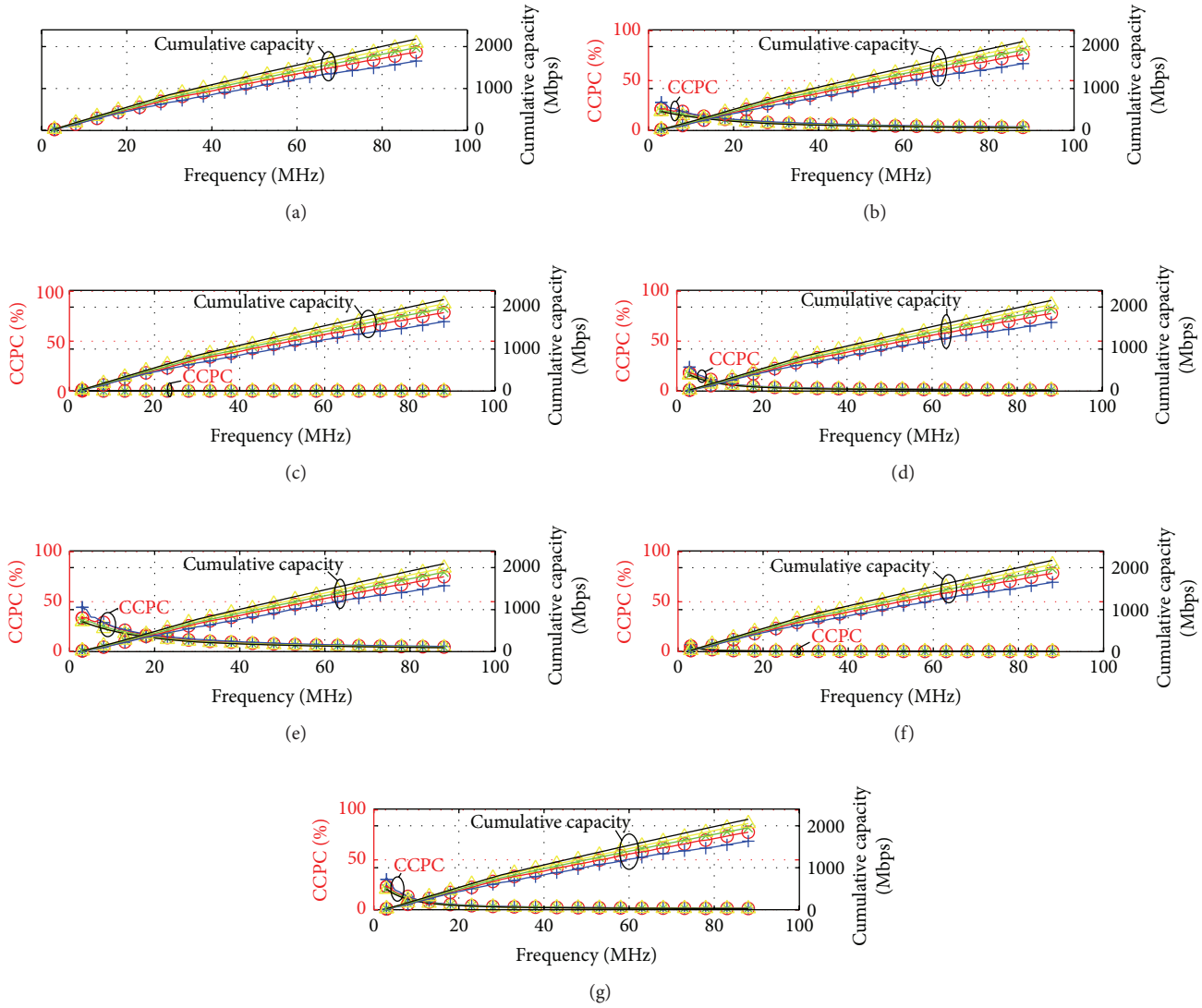

Figure 8: The same as in Figure 5, but for UN LV BPL networks.

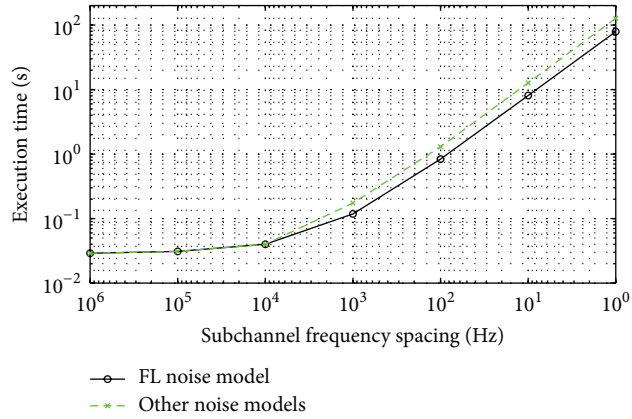

Figure 9: The execution time of the seven noise models in the 3–88 MHz frequency range for different flat-fading subchannel frequency spacing.

StP: Shield-to-Phase
SVD: Singular Value Decomposition
TM2 method: T-Matrix 2 method
UN: Underground
WtG: Wire-to-Ground
WtW: Wire-to-Wire
XLPE: Cross-Linked PolyEthylene.

Conflict of Interests

The author declares that there is no conflict of interests regarding the publication of this paper.

References

[1] A. G. Lazaropoulos and P. G. Cottis, "Transmission characteristics of overhead medium-voltage power-line communication channels," *IEEE Transactions on Power Delivery*, vol. 24, no. 3, pp. 1164–1173, 2009.

[2] A. G. Lazaropoulos and P. G. Cottis, "Capacity of overhead medium voltage power line communication channels," *IEEE Transactions on Power Delivery*, vol. 25, no. 2, pp. 723–733, 2010.

[3] A. G. Lazaropoulos and P. G. Cottis, "Broadband transmission via underground medium-voltage power lines—part I: transmission characteristics," *IEEE Transactions on Power Delivery*, vol. 25, no. 4, pp. 2414–2424, 2010.

[4] A. G. Lazaropoulos and P. G. Cottis, "Broadband transmission via underground medium-voltage power lines—part II: capacity," *IEEE Transactions on Power Delivery*, vol. 25, no. 4, pp. 2425–2434, 2010.

[5] A. G. Lazaropoulos, "Towards broadband over power lines systems integration: transmission characteristics of underground low-voltage distribution power lines," *Progress in Electromagnetics Research B*, vol. 39, pp. 89–114, 2012, http://www.jpier.org/PIERB/pierb39/05.12012409.pdf.

[6] A. G. Lazaropoulos, "Towards modal integration of overhead and underground low-voltage and medium-voltage power line communication channels in the smart grid landscape: model expansion, broadband signal transmission characteristics, and statistical performance metrics (invited paper)," *ISRN Signal Processing*, vol. 2012, Article ID 121628, 17 pages, 2012.

[7] S. Galli, A. Scaglione, and Z. Wang, "For the grid and through the grid: the role of power line communications in the smart grid," *Proceedings of the IEEE*, vol. 99, no. 6, pp. 998–1027, 2011.

[8] A. G. Lazaropoulos, "Numerical evaluation of broadband transmission characteristics of underground low-voltage networks—introducing techno-pedagogical (TP) method," *International Journal of Electrical Power & Energy Systems*, vol. 55, pp. 253–260, 2014.

[9] A. G. Lazaropoulos, "Wireless sensor network design for transmission line monitoring, metering, and controlling: introducing broadband over power lines-enhanced network model (BPLeNM)," *ISRN Power Engineering*, vol. 2014, Article ID 894628, 22 pages, 2014.

[10] M. Gebhardt, F. Weinmann, and K. Dostert, "Physical and regulatory constraints for communication over the power supply grid," *IEEE Communications Magazine*, vol. 41, no. 5, pp. 84–90, 2003.

[11] S. Liu and L. J. Greenstein, "Emission characteristics and interference constraint of overhead medium-voltage broadband power line (BPL) systems," in *Proceedings of the IEEE Global Telecommunications Conference (IEEE GLOBECOM '08)*, pp. 1–5, IEEE, New Orleans, LA, USA, November-December 2008.

[12] D. Fenton and P. Brown, "Modelling cumulative high frequency radiated interference from power line communication systems," in *Proceedings of the IEEE International on Power Line Communications and Its Applications (ISPLC '02)*, Athens, Greece, March 2002.

[13] A. G. Lazaropoulos, "Review and progress towards the capacity boost of overhead and underground medium-voltage and low-voltage broadband over power lines networks: cooperative communications through two- and three-hop repeater systems," *ISRN Electronics*, vol. 2013, Article ID 472190, 19 pages, 2013.

[14] M. Zimmermann and K. Dostert, "Analysis and modeling of impulsive noise in broad-band powerline communications," *IEEE Transactions on Electromagnetic Compatibility*, vol. 44, no. 1, pp. 249–258, 2002.

[15] D. Benyoucef, "A new statistical model of the noise power density spectrum for powerline communications," in *Proceedings of the IEEE 7th International Symposium on Power-Line Communications and its Applications (ISPLC '03)*, pp. 136–141, Kyoto, Japan, March 2003.

[16] N. Andreadou and F.-N. Pavlidou, "Modeling the noise on the OFDM power-line communications system," *IEEE Transactions on Power Delivery*, vol. 25, no. 1, pp. 150–157, 2010.

[17] OPERA1. D5, "Pathloss as a function of frequency, distance and network topology for various LV and MV European powerline networks," IST Integrated Project 507667, 2005.

[18] Ofcom, "Ascom PLT measurements in Winchester," Tech. Rep. 793 (Part 1), Ofcom, London, UK, 2005.

[19] J. Song, C. Pan, Q. Wu et al., "Field trial of digital video transmission over medium-voltage powerline with time-domain synchronous orthogonal frequency division multiplexing technology," in *Proceedings of the IEEE International Symposium on Power Line Communications and Its Applications (ISPLC '07)*, pp. 559–564, Pisa, Italy, March 2007.

[20] H. Meng, Y. L. Guan, and S. Chen, "Modeling and analysis of noise effects on broadband power-line communications," *IEEE Transactions on Power Delivery*, vol. 20, no. 2, pp. 630–637, 2005.

[21] V. Degardin, M. Lienard, A. Zeddam, F. Gauthier, and P. Degauque, "Classification and characterization of impulsive noise on indoor power line used for data communications," *IEEE Transactions on Consumer Electronics*, vol. 48, no. 4, pp. 913–918, 2002.

[22] H. Hrasnica, A. Haidine, and R. Lehnert, *Broadband Powerline Communications: Network Design*, John Wiley & Sons, Hoboken, NJ, USA, 2004.

[23] H. Philipps, "Development of a statistical model for powerline communications channels," in *Proceedings of the 4th International Symposium on Power-Line Communications and Its Applications (ISPLC '00)*, IEEE, Limerick, Ireland, April 2000.

[24] J. Meng and A. E. Marble, "Effective communication strategies for noise-limited power-line channels," *IEEE Transactions on Power Delivery*, vol. 22, no. 2, pp. 887–892, 2007.

[25] V. Degardin, M. Lienard, and P. Degauque, "Transmission on indoor power lines: from a stochastic channel model to the optimization and performance evaluation of multicarrier systems," *International Journal of Communication Systems*, vol. 16, no. 5, pp. 363–379, 2003.

[26] T. Esmailian, F. R. Kschischang, and P. G. Gulak, "In-building power lines as high-speed communication channels: channel characterization and a test channel ensemble," *International*

Journal of Communication Systems, vol. 16, no. 5, pp. 381–400, 2003.

[27] J. Meng, "Noise analysis of power-line communications using spread-spectrum modulation," *IEEE Transactions on Power Delivery*, vol. 22, no. 3, pp. 1470–1476, 2007.

[28] J. Zhang and J. Meng, "Noise resistant OFDM for power-line communication systems," *IEEE Transactions on Power Delivery*, vol. 25, no. 2, pp. 693–701, 2010.

[29] P. Amirshahi and M. Kavehrad, "High-frequency characteristics of overhead multiconductor power lines for broadband communications," *IEEE Journal on Selected Areas in Communications*, vol. 24, no. 7, pp. 1292–1302, 2006.

[30] T. Calliacoudas and F. Issa, "'Multiconductor transmission lines and cables solver', an efficient simulation tool for PLC channel networks development," in *Proceedings of the IEEE International Conference on Power Line Communications and Its Applications*, Athens, Greece, March 2002.

[31] S. Galli and T. C. Banwell, "A deterministic frequency-domain model for the indoor power line transfer function," *IEEE Journal on Selected Areas in Communications*, vol. 24, no. 7, pp. 1304–1316, 2006.

[32] T. Sartenaer and P. Delogne, "Deterministic modeling of the (shielded) outdoor power line channel based on the multiconductor transmission line equations," *IEEE Journal on Selected Areas in Communications*, vol. 24, no. 7, pp. 1277–1291, 2006.

[33] C. R. Paul, *Analysis of Multiconductor Transmission Lines*, John Wiley & Sons, New York, NY, USA, 1994.

[34] Y.-H. Kim, S. Choi, S.-C. Kim, and J.-H. Lee, "Capacity of OFDM two-hop relaying systems for medium-voltage power-line access networks," *IEEE Transactions on Power Delivery*, vol. 27, no. 2, pp. 886–894, 2012.

[35] P. Amirshahi, *Broadband access and home networking through power-line networks [Ph.D. thesis]*, Pennsylvania State University, University Park, Pa, USA, 2006, http://etda.libraries.psu.edu/theses/approved/WorldWideIndex/ETD-1205/index.html.

[36] P. Amirshahi and M. Kavehrad, "Medium voltage overhead power-line broadband communications; transmission capacity and electromagnetic interference," in *Proceedings of the 9th International Symposium on Power Line Communications and Its Applications (ISPLC '05)*, pp. 2–6, IEEE, Vancouver, Canada, April 2005.

[37] OPERA1, "D44: report presenting the architecture of PLC system, the electricity network topologies, the operating modes and the equipment over which PLC access system will be installed," IST Integrated Project 507667, 2005.

[38] A. G. Lazaropoulos, "Broadband over power lines systems convergence: multiple-input multiple-output communications analysis of overhead and underground low-voltage and medium-voltage BPL Networks," *ISRN Power Engineering*, vol. 2013, Article ID 517940, 30 pages, 2013.

[39] M. D'Amore and M. S. Sarto, "Simulation models of a dissipative transmission line above a lossy ground for a wide-frequency range—part I: single conductor configuration," *IEEE Transactions on Electromagnetic Compatibility*, vol. 38, no. 2, pp. 127–138, 1996.

[40] M. D'Amore and M. S. Sarto, "Simulation models of a dissipative transmission line above a lossy ground for a wide-frequency range—Part II: multiconductor configuration," *IEEE Transactions on Electromagnetic Compatibility*, vol. 38, no. 2, pp. 139–149, 1996.

[41] P. C. J. M. van der Wielen, *On-line detection and location of partial discharges in medium-voltage power cables [Ph.D. dissertation]*, Technische Universiteit Eindhoven, Eindhoven, Netherlands, 2005, http://alexandria.tue.nl/extra2/200511097.pdf.

[42] M. Tang and M. Zhai, "Research of transmission parameters of four-conductor cables for power line communication," in *Proceedings of the International Conference on Computer Science and Software Engineering*, vol. 5, pp. 1306–1309, Wuhan, China, December 2008.

[43] N. Theethayi, *Electromagnetic interference in distributed outdoor electrical systems, with an emphasis on lightning interaction with electrified railway network [Ph.D. thesis]*, Uppsala University, Uppsala, Sweden, 2005.

[44] J. Anatory, N. Theethayi, R. Thottappillil, M. M. Kissaka, and N. H. Mvungi, "The effects of load impedance, line length, and branches in typical low-voltage channels of the BPLC systems of developing countries: transmission-line analyses," *IEEE Transactions on Power Delivery*, vol. 24, no. 2, pp. 621–629, 2009.

[45] Ofcom, "Amperion PLT measurements in Crieff," Tech. Rep., Ofcom, London, UK, 2005.

[46] NATO, "HF interference, procedures and tools," Final Report of NATO RTO Information Systems Technology RTO-TR-ISTR-050, 2007, http://ftp.rta.nato.int/public/PubFullText/RTO/TR/RTO-TR-IST-050/$$TR-IST-050-ALL.pdf.

[47] FCC, "In the matter of amendment of part 15 regarding new requirements and measurement guidelines for access broadband over power line systems," FCC 04-245, Report and Order, 2008.

[48] M. V. Ribeiro, R. da Rocha Lopes, J. M. T. Romano, and C. A. Duque, "Impulse noise mitigation based on computational intelligence for improved bit rate in PLC-DMT," *IEEE Transactions on Power Delivery*, vol. 21, no. 1, pp. 94–101, 2006.

[49] T. A. Papadopoulos, C. G. Kaloudas, A. I. Chrysochos, and G. K. Papagiannis, "Application of narrowband power-line communication in medium-voltage smart distribution grids," *IEEE Transactions on Power Delivery*, vol. 28, no. 2, pp. 981–988, 2013.

[50] T. A. Papadopoulos, A. I. Chrysochos, and G. K. Papagiannis, "Narrowband power line communication: medium voltage cable modeling and laboratory experimental results," *Electric Power Systems Research*, vol. 102, pp. 50–60, 2013.